View metadata, citation and similar papers at core.ac.uk
brought to you by CORE
provided by ScholarWorks@UNIST

PHYSICAL REVIEW B **83**, 125319 (2011)

Dirac cone engineering in Bi_2Se_3 thin films

Hosub Jin, Jung-Hwan Song,* and Arthur J. Freeman
Department of Physics and Astronomy, Northwestern University, Evanston, Illinois 60208, USA
(Received 14 May 2010; revised manuscript received 1 February 2011; published 29 March 2011)

In spite of the clear surface-state Dirac cone features in bismuth-based three-dimensional strong topological insulator materials, the Dirac point known as the Kramers point and the topological transport regime are located near the bulk valence band maximum. As a result of a nonisolated Dirac point, the topological transport regime cannot be acquired and there possibly exist scattering channels between surface and bulk states as well. We show that an ideal and isolated Dirac cone is realized in a slab geometry made of Bi_2Se_3 with appropriate substitutions of surface Se atoms. As an extension of Dirac cone engineering, we also investigate Bi_2Se_3 ultrathin films with asymmetric or magnetic substitutions of the surface atoms, which can be linked to spintronics applications.

DOI: 10.1103/PhysRevB.83.125319 PACS number(s): 71.20.−b, 73.20.At, 73.22.−f

Topologically protected surface or edge states, free of back-scattering, and spin-momentum locked massless Dirac cones are key features of topological insulators (TI),[1,2] from which it is possible to realize a number of new applications and new fundamental physical phenomena such as fault-tolerant quantum computing and the anomalous quantization of magnetic-electric coupling.[3,4] To utilize their distinctive properties and applications, TI should be tuned in such a way that the ideal and isolated Dirac cones, i.e., the topological transport regime, should be easily accessible without any scattering channels. The topological transport regime can perhaps be best demonstrated by bismuth-based compounds such as Bi_2Se_3 and Bi_2Te_3, which were discovered by recent theoretical and experimental studies[5,6] and have one simple surface-state Dirac cone at the Γ point. However, according to previous first-principles calculations,[5,7,8] clean surfaces of these materials have the topological transport regime located below or very close to the bulk valence band maximum, and thus a vanishing density of states at the Dirac point cannot be readily achieved, which is crucial for manifesting novel phenomena such as an anomalous half-integer quantization of Hall conductance. This situation also possibly introduces multiple-scattering sources. The surface states within the valence bands have scattering channels with bulk states.[9,10] The surface states of the Dirac cone far from the Dirac point show hexagram isoenergy contours rather than circular ones in the two-dimensional Brillouin zone, which is also a scattering channel at certain nesting vectors.[11,12] Apart from the scattering sources in which only a single surface is involved, one more important scattering source is the intersurface interaction from two opposing surfaces in a very thin film geometry.[13,14] The intersurface interaction in this case develops a small gap at the Dirac point.

Here we use a first-principles all-electron approach[15] to investigate the effect of substitutions at the surface layer, the intersurface interactions in an asymmetric Bi_2Se_3 slab, and finally the role of magnetic dopants. We propose substitutions at the surface layer to manipulate the level of the Dirac point relative to the valence band maximum, which may result in an isolated topological transport regime. Tuning the Dirac cone in Bi_2Se_3 was first demonstrated experimentally by Hsieh *et al.*,[16] and our theoretical work is consistent in suggesting another way for tuning and explaining its mechanisms. With Dirac cone engineering using the surface atom substitution and exploiting the intersurface interaction in TI thin films, we calculated Bi_2Se_3 ultrathin films with asymmetric substitution and found consistent results with the previous experimental and theoretical work of Bi_2Se_3 thin films grown on SiC substrate.[14,17] Here, the form of the resulting Hamiltonian composed of two asymmetric surface states, the so-called double Rashba Hamiltonian, is introduced. The double Rashba Hamiltonian is an extension of the normal Rashba model, containing both electron and hole excitations, and thus can show the opposite sign of spin Hall conductivity. We also demonstrate that magnetic-ion substitution opens a gap in the Dirac cone of a single surface,[18] which gives rise to the absence of the intersurface interaction and finally recovers a single Dirac cone at the opposite surface in the ultrathin films.

Depending on the treatment of the surface layers proposed here, manipulation of the Dirac cone and the intersurface interactions will, yield ideal coherent spin transport utilizing a single surface of ultra thin films or *p*- and *n*-type spin currents in a single thin film from intrinsic double Rashba effects. This opens new technological opportunities such as spin-polarized *p*-*n* junction devices, including electrical control of spin Hall conductivities.

To determine the electronic structures and to optimize the geometry, the first-principles calculations were performed using the highly precise full-potential linearized augmented plane-wave (FLAPW)[15] method with the gradient-corrected Perdew, Burke, and Ernzerhof form of the exchange-correlation potential. The calculations were carried out with the experimental lattice parameters for in-plane, but the internal atomic coordinates were fully optimized. The core states and the valence states were treated fully relativistically and scalar relativistically, respectively. The spin-orbit coupling was included by a second variational procedure.[19]

Despite a Dirac cone dispersion of the pristine Bi_2Se_3 slab shown in Fig. 1(a), its Dirac point is quite close to the bulk states and both Dirac point and bulk states appear at the same energy level, which can be a source of scattering. Elastic impurity scattering between surface states and bulk states was detected in recent scanning tunneling microscopy and scanning tunneling spectroscopy experiments on a Sb (1 1 1) surface.[10] Meanwhile, the linear part of the surface state inside the bulk band gap region shows a hexagram shape

 ©2011 American Physical Society

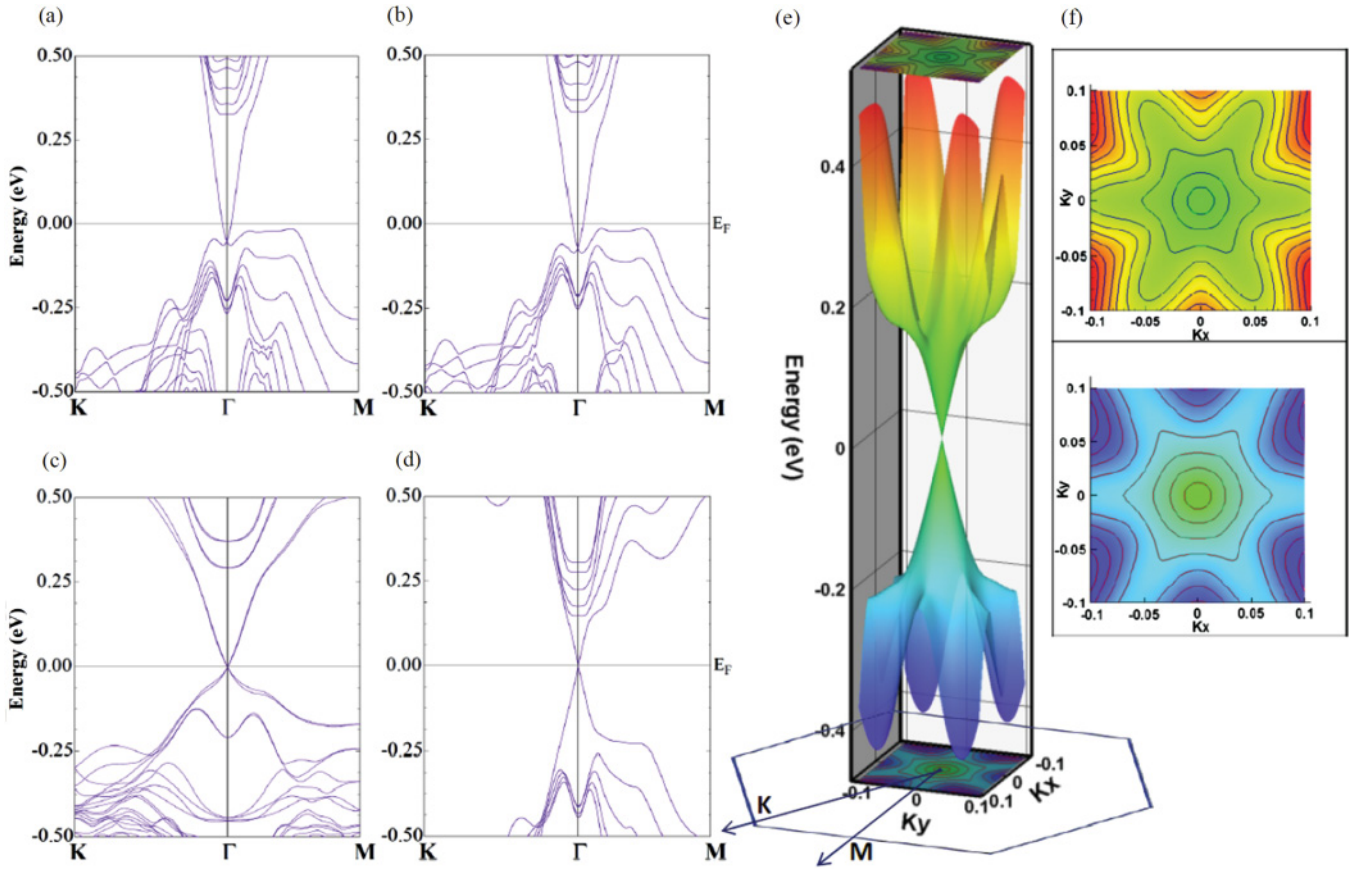

FIG. 1. (Color online) Quasiparticle dispersions of (a) a Bi_2Se_3 pristine slab, (b) a Bi_2Se_3 slab with S substitutions of end Se atoms, and a Bi_2Se_3 slab with (c) 50% and (d) 100% O substitutions. All film geometries consist of 1×1 on the *ab* plane and six quintuple layers except for the case of 50% O substitutions consisting of 2×2 and three quintuple layers. (e) Three-dimensional plot of the surface state from O-substituted case in (d), and (f) its contour plot above and below the Dirac point.

of isoenergy contours around the Γ point in the hexagonal surface Brillouin zone, where other finite $\vec{\mathbf{q}}$ elastic scattering channels are possible.

By appropriate substitutions at the surface, the changes in the surface potential affect the level of surface state and finally we can acquire the ideal Dirac cone which is placed inside the bulk band gap of Bi_2Se_3. When we substitute S or O for the surface Se atom at both ends of the Bi_2Se_3 film, the topologically protected surface state connecting the inverted bulk conduction and valence bands moves differently. When S is substituted, no significant change in the surface state occurs, as shown in Fig. 1(b). In the case of O substitutions, an ideal and isolated Dirac cone with pointlike Fermi surface at Γ is realized [Fig. 1(c)–1(f)]; Figs. 1(c) and 1(d) are the electronic band structures with 50 and 100% O substitutions of the surface Se atoms, respectively. Comparing three different surface coverages of oxygen atoms (0, 50, and 100%), the position of the Dirac point relative to the bulk valence bands moves upward as the coverage ratio increases. From these results, we can get a hint to tune the position of the Dirac point continuously by controlling the amount of O substitutions. As shown in Figs. 1(e) and 1(f), there is a circular cross section to the isoenergy contour in the energy range of $\sim\pm 0.1$ eV above and below the Fermi level which is free from scattering originating from the bulk states or the hexagram cross section. At the same time, electron-hole symmetry of the Dirac cone is shown in this energy range. Due to the lack of bulk states near the Dirac point, the Fermi level pinned at the Dirac point in the neutral system can be easily manipulated by chemical doping or gate voltage.[16] Scanning tunneling spectroscopy measurements on the O-substituted TI surface should not show any spatial oscillations at certain scattering wave-vectors in the energy range inside the Bi_2Se_3 band gap. The ideal Dirac cone of the surface state is a good starting point to realize intriguing quantum phenomena suggested by the model Hamiltonian, which emphasize the importance of the topological transport regime. Recent experiments on TI thin films using molecular beam epitaxy[14] might be useful to realize the suggested configurations here.[20]

Redistribution of the charge density of the surface states is closely related to the shift of the Dirac cone level. With the atomic positions, the charge-density plots of the surface states at Γ are depicted in Fig. 2. A large amount of the surface state in the O-substituted case resides in two Se atoms facing each other at the boundary of neighboring quintuple layers [Fig. 2(c)], whereas in the other cases, the surface state spreads throughout the outermost quintuple layers [Figs. 2(a) and 2(b)]. When O replaces Se, it strongly binds with, and shrinks toward, the Bi, making nearly a perfect single layer of O and Bi. Strongly bonded O-Bi layers form a band insulator region within the quintuple layer,[21] and the surface state is pushed down to the boundary with the neighboring quintuple layer.

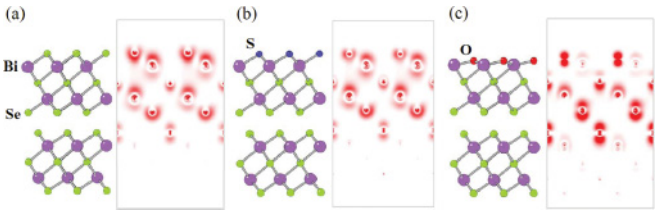

FIG. 2. (Color online) Charge-density plots of the surface states at Γ (a) from a Bi_2Se_3 pristine slab, (b) with S substitution, and (c) with O substitution.

Due to the confinement of the surface state within the narrow region, the Dirac cone energy level moves upward and the Dirac point appears inside the bulk band gap region.

For applications such as 2D electronic devices, the investigation of the physical properties of TI thin films where two surfaces are separated by several nanometers are needed. Considering a free standing slab of Bi_2Se_3 with n quintuple layers where n is in the range from 1 to 6, there is a gap at the Γ point, and no surface state crossing of the Fermi level to connect the conduction and valence bands. As n increases, the gap decreases down to sub-meV at $n = 6$, in agreement with previous work.[22] The origin of these small gaps is the interaction between surface states from opposite surfaces of the slab. For the finite TI slab, scattering between the two surface states from the opposing surfaces with the opposite momentum, but the same spin is allowed which creates a small gap at the crossing point even though the scattering between the Kramers pair at the same surface is still forbidden.[23]

Based on the fact that substitutions of the surface anion change the energy level of the surface state Dirac cone, we suggest an asymmetric ultrathin TI slab by replacing atoms at the end of one surface to generate an asymmetric potential and to break the degeneracy between surface states from each side. By substitution of S and O for Se in three quintuple Bi_2Se_3 layers, we acquired two different surface states whose Dirac points at Γ do not coincide. There still exist intersurface interactions between channels with the same spin from opposing sides, but the gap opens slightly off Γ because the crossing points between the scattering channels are shifted due to the asymmetric environment. As a result of the asymmetric potential and intersurface interaction, a gap is opened at those crossing points, but two gapless Dirac points from asymmetric surfaces are placed at different energy levels at Γ.

The asymmetric thin film has the advantage of carrying finite spin Hall currents whose magnitude and direction are determined by the position of the chemical potential. For symmetric geometries, even though each topologically protected surface state carries spin Hall currents, they are exactly canceled out by those from the opposing sides of the film. However, in the case of an asymmetric slab, we can expect a finite spin Hall conductivity due to imperfect cancellation. Starting from two surface states described by a helical Dirac Hamiltonian and asymmetric potential V_a, the model Hamiltonian H can be built to consider the intersurface interactions V_I.

$$H = \left[\frac{V_a}{2}\sigma_0 + v_F\vec{\sigma}\cdot(\hat{z}\times\vec{p})\right]\tau_3 + V_I\sigma_0\tau_1, \qquad (1)$$

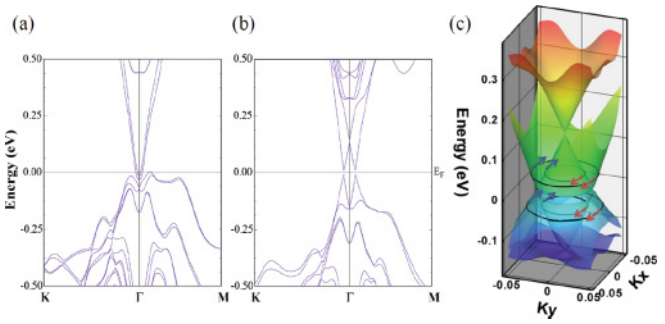

FIG. 3. (Color online) Electronic band structures of three quintuple layers consisting of Bi_2Se_3 slab with (a) S and (b) O substitution. (c) Three-dimensional plots of band structure in (b). Considering the spin directions in momentum space (denoted as arrows), two asymmetric surface states with intersurface interaction adiabatically connect to the double Rashba model.

where σ_0 is the 2×2 unit matrix and σ_i and τ_i are Pauli matrices indicating spin and surfaces respectively. By using an unitary transformation[24] to fold back the off-diagonal component V_I and expanding up to $(V_I/V_a)^2$, H can be written as

$$\widetilde{H} = e^{-S}He^{S} = \left[\left(\frac{\widetilde{V}_a}{2} + \frac{p^2}{2\widetilde{m}}\right)\sigma_0 + \widetilde{v}_F\vec{\sigma}\cdot(\hat{z}\times\vec{p})\right]\tau_3, \qquad (2)$$

which is exactly mapped into the Rashba Hamiltonian. The asymmetric potential ($\widetilde{V}_a$) generated by O substitution is 0.29 eV, which is larger than that from Bi_2Se_3 thin films on the SiC substrate.[14,17] Again, it shows that we can tune the asymmetric potential by changing the oxygen surface-coverage ratio.

Considering the band dispersions of the surface state induced by intersurface interactions, and helical spin textures in momentum space [Fig. 3(c)], the band dispersions are adiabatically connected to the Rashba Hamiltonian so they give a nonzero spin Hall conductance.[25] More importantly, $\widetilde{H}$ is composed of a double Rashba model where the same Hamiltonian is applied both for electron and hole excitations. Due to the characteristics of electron and hole excitations for surface-state bands above and below the gap, the sign of the spin Hall conductivity is changed when the Fermi level is shifted across the gap. Therefore, the direction of spin Hall currents can be easily reversed by adjusting the chemical potential.

A way to avoid intersurface interaction and to recover a gapless surface state in finite TI thin films is to destroy one surface state by exerting a local magnetic field limited only to one surface and breaking local time-reversal symmetry which makes a gap at the Dirac point of the surface state. Due to gapping one surface state, the other surface state is free from scattering at the Dirac point and has gapless dispersions even in thinner Bi_2Se_3 films where there are intersurface gaps at the Dirac point. To generate a magnetic field localized on one surface of the Bi_2Se_3 thin film, we set up an asymmetric slab with substitution of the end Bi-Se sublayer by Mn and I (MnI). With MnI replacement, Mn has a $3d^5$ configuration where we can make use of its large

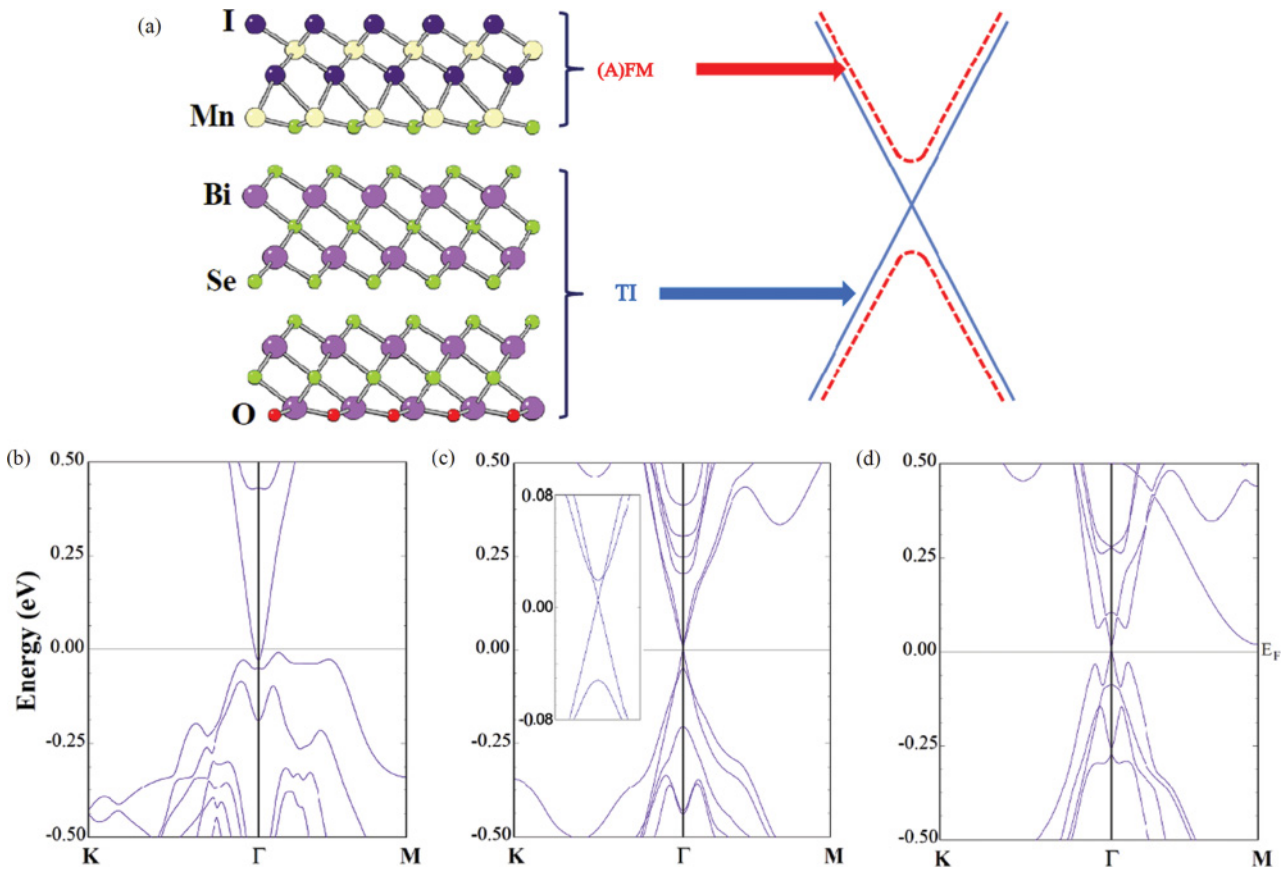

FIG. 4. (Color online) Crystal structure of three quintuple layers of Bi_2Se_3 with O substitution at one end and (MnI) substitution at the other end. Schematic band dispersions comparing two different surface states from the O-substituted side (blue, gapless) and from the (MnI)-substituted side (red, finite gap). Band structures of three quintuple layers of (b) a pristine Bi_2Se_3 slab, (c) O and (MnI) substitutions at both ends, and (d) O and $(MnI)_2$ substitutions.

magnetic moment and exchange splitting to open a gap at the Dirac point at one surface state. To calculate this system, we adopted the LDA+U scheme containing spin-orbit interaction with $U = 4.0$ eV and $J = 1.0$ eV for the Mn $3d$ orbitals. With this stoichiometric substitution, the calculated magnetic moments are nearly 5-bohr magnetons per Mn regardless of U. More importantly, MnI substitution not only generates a local magnetic field but also plays the role of an asymmetric potential to shift the surface state upward, similar to the case of O substitution. Even though a single gapless Dirac cone in the Bi_2Se_3 thin film under local magnetic fields is realized, its Dirac point is not isolated from other states. To obtain an isolated single Dirac cone through the whole Brillouin zone in a certain energy window inside not only the bulk gap but also the surface-state gap generated by a local field, we set up a three-quintuple layer Bi_2Se_3 slab with MnI and O substitution for each surface. By O substitution, the energy level of a gapless surface state moves upward and is just located inside the gap of the other surface state opened by the local magnetic field. As shown in Fig. 4(c), we can identify two different surface states, where one is gapped by 69 meV at Γ and the other is gapless. The energy window of an isolated Dirac cone is limited by the gap of the MnI-substituted surface state. Making thicker magnetic layers by $(MnI)_2$ substitution, the surface-state gap induced by the magnetic field grows [Fig. 4(d)]. Since it is preferable to have a large energy window for practical use, the possibilities of enlarging the gap by utilizing different configurations with different ferromagnetic materials should be investigated in the future. One important implication of destroying one surface state and avoiding the intersurface interaction is that we can make an ultrathin film which preserves a gapless and isolated surface state.

Isolated and ideal Dirac cone surface states, protected by time-reversal symmetry, will play an important role in charge and spin transport experiments with their long coherent length and high mobility. Dirac cone engineering done by the substitutions of surface atoms which alters the level of surface states without changing the bulk states can also be applicable to another promising three-dimensional TI, Bi_2Te_3. Asymmetric substitutions with magnetic or nonmagnetic ions in the Bi_2Se_3 narrow slab showed various applicability by using the helical Dirac fermions of the surface states and the interactions between them which are inevitable in thin film geometries of the TI.

Financial support from the US DOE under Grant No. DE-FG02-88ER45372 is gratefully acknowledged.

*Corresponding author: jhsong@pluto.phys.northwestern.edu

[1] M. Z. Hasan and C. L. Kane, Rev. Mod. Phys. **82**, 3045 (2010).
[2] X.-L. Qi and S.-C. Zhang, Phys. Today **63**, 33 (2010).
[3] L. Fu and C. L. Kane, Phys. Rev. Lett. **100**, 096407 (2008).
[4] X.-L. Qi, R. Li, J. Zang, and S.-C. Zhang, Science **323**, 1184 (2009).
[5] Y. Xia, D. Qian, D. Hsieh, L. Wray, A. Pal, H. Lin, A. Bansil, D. Grauer, Y. S. Hor, R. J. Cava, and M. Z. Hasan, Nat. Phys. **5**, 398 (2009).
[6] H. Zhang, C.-X. Liu, X.-L. Qi, X. Dai, Z. Fang, and S.-C. Zhang, Nat. Phys. **5**, 438 (2009).
[7] D. Hsieh, Y. Xia, D. Qian, L. Wray, F. Meier, J. H. Dil, J. Osterwalder, L. Patthey, A. V. Fedorov, H. Lin, A. Bansil, D. Grauer, Y. S. Hor, R. J. Cava, and M. Z. Hasan, Phys. Rev. Lett. **103**, 146401 (2009).
[8] W. Zhang, R. Yu, H.-J. Zhang, X. Dai, and Z. Fang, New J. Phys. **12**, 065013 (2010).
[9] P. Roushan, J. Seo, C. V. Parker, Y. S. Hor, D. Hsieh, D. Qian, A. Richardella, M. Z. Hasan, R. J. Cava, and A. Yazdani, Nature **460**, 1106 (2009).
[10] K. K. Gomes, W. Ko, W. Mar, Y. Chen, Z. Shen, and H. C. Manoharan, e-print arXiv:0909.0921.
[11] Y. L. Chen, J. G. Analytis, J.-H. Chu, Z. K. Liu, S.-K. Mo, X. L. Qi, H. J. Zhang, D. H. Lu, X. Dai, Z. Fang, S. C. Zhang, I. R. Fisher, Z. Hussain, and Z.-X. Shen, Science **325**, 178 (2009).
[12] L. Fu, Phys. Rev. Lett. **103**, 266801 (2009).
[13] B. Zhou, H.-Z. Lu, R.-L. Chu, S.-Q. Shen, and Q. Niu, Phys. Rev. Lett. **101**, 246807 (2008).
[14] Y. Zhang, K. He, C.-Z. Chang, C.-L. Song, L. Wang, X. Chen, J. Jia, Z. Fang, X. Dai, W.-Y. Shan, S.-Q. Shen, Q. Niu, X. Qi, S.-C. Zhang, X. Ma, and Q.-K. Xue, Nat. Phys. **6**, 584 (2010).
[15] E. Wimmer, H. Krakauer, M. Weinert, and A. J. Freeman, Phys. Rev. B **24**, 864 (1981).
[16] D. Hsieh, Y. Xia, D. Qian, L. Wray, J. H. Dil, F. Meier, J. Osterwalder, L. Patthey, J. G. Checkelsky, N. P. Ong, A. V. Fedorov, H. Lin, A. Bansil, D. Grauer, Y. S. Hor, R. J. Cava, and M. Z. Hasan, Nature **460**, 1101 (2009).
[17] W.-Y. Shan, H.-Z. Lu, and S.-Q. Shen, New J. Phys. **12**, 043048 (2010).
[18] Y. S. Hor, P. Roushan, H. Beidenkopf, J. Seo, D. Qu, J. G. Checkelsky, L. A. Wray, D. Hsieh, Y. Xia, S.-Y. Xu, D. Qian, M. Z. Hasan, N. P. Ong, A. Yazdani, and R. J. Cava, Phys. Rev. B **81**, 195203 (2010).
[19] A. H. MacDonald, W. E. Pickett, and D. D. Koelling, J. Phys. C **13**, 2675 (1980).
[20] To investigate the possibility of oxygen substitutions, we calculated the formation energy in 50 and 100% oxygen replacement of surface Se atoms. The formation energy, written as $E_f = E_{\mathrm{O-sub}} - E_{\mathrm{pristine}} + n_{\mathrm{Se}}\mu_{\mathrm{Se}} - n_{\mathrm{O}}\mu_{\mathrm{O}}$, can vary in the thermodynamically allowed range $\mu_{\mathrm{Se}}^{\mathrm{bulk}} + \Delta H_f \leqslant \mu_{\mathrm{Se}} \leqslant \mu_{\mathrm{Se}}^{\mathrm{bulk}}$, where ΔH_f is the heat of formation of bulk Bi_2Se_3. Here, μ_{O} is obtained from the O_2 molecule, and the temperature and pressure dependence of reservoirs is taken into account using $\mu_{\mathrm{O}} = E_{\mathrm{O}_2}/2 + k_B T \ln(pV_Q/k_B T)$, where $V_Q = (h^2/2\pi m k_B T)^{\frac{3}{2}}$. (See Ref. 26.) With the molecular beam epitaxy growth conditions, $T =$ 600 K, and $p = 10^{-6}$ Torr, the estimated values are -0.20 eV $\leqslant E_f(100\%) \leqslant 0.42$ eV and -0.32 eV $\leqslant E_f(50\%) \leqslant 0.31$ eV, respectively.
[21] J.-H. Song, H. Jin, and A. J. Freeman, Phys. Rev. Lett. **105**, 096403 (2010).
[22] C.-X. Liu, H. J. Zhang, B. Yan, X.-L. Qi, T. Frauenheim, X. Dai, Z. Fang, and S.-C. Zhang, Phys. Rev. B **81**, 041307 (2010).
[23] C. L. Kane and E. J. Mele, Phys. Rev. Lett. **95**, 226801 (2005).
[24] R. Winkler, *Spin-Orbit Coupling Effects in Two-Dimensional Electron and Hole Systems* (Springer-Verlag, Berlin, 2003).
[25] J. Sinova, D. Culcer, Q. Niu, N. A. Sinitsyn, T. Jungwirth, and A. H. MacDonald, Phys. Rev. Lett. **92**, 126603 (2004).
[26] T. Akiyama, K. Nakamura, T. Ito, J.-H. Song, and A. J. Freeman, Phys. Rev. B **80**, 075316 (2009).